

Testing the Noncommutative Standard Model at a Future Photon Collider

Thorsten Ohl^{a,*}, Jürgen Reuter^{b,†}

^a Institut für Theoretische Physik und Astrophysik,
Universität Würzburg, D-97074 Würzburg, Germany

^b Institut für Theoretische Teilchenphysik,
Universität Karlsruhe, D-76128 Karlsruhe, Germany

February 22, 2019

WUE-ITP-2003-020	TTP 03-25	hep-ph/04xxxxx
------------------	-----------	----------------

Abstract

Extensions of the Standard Model of elementary particle physics to noncommutative geometries have been proposed as a low energy limit of string models. Independent of this motivation, one may consider such a model as an effective field theory with higher-dimensional operators containing an antisymmetric rank-two background field. We study the signals of such a Noncommutative Standard Model (NCSM) and analyze the discovery potential of a future photon collider considering angular distributions in fermion pair production.

Keywords Noncommutative Field Theory, Polarization, Photon Collider, Helicity Amplitudes, Spinor Products

PACS 11.10.Nx, 11.30.Cp, 11.80.Cr, 13.88.+e, 13.90.+i

*email: ohl@physik.uni-wuerzburg.de

†email: reuter@particle.uni-karlsruhe.de

1 Introduction

The idea of noncommutative space-time coordinates is more than half a century old. However, interest in noncommutative (NC) theories has been growing dramatically in recent years due to the observation that open string theories with constant antisymmetric rank-two tensor background fields in the limit of vanishing string tension $\alpha' \rightarrow 0$ can be interpreted as Yang-Mills theories living on a NC manifold [1]. Independent of this motivation provided by string theory, Noncommutative Quantum Field Theory (NCQFT) in itself provides an interesting approach to introducing a fundamental length scale and consequently cutting off short-distance contributions in a way that is consistent with the symmetries of a given model.

Although there still remain open questions regarding the definition and consistency of perturbative NCQFTs (e.g. UV/IR mixing [2] and unitarity [3]) one can study a particular NC structure and its phenomenological consequences. This will be the scope of the present paper.

Recently, there has been a lot of activity in model building, trying to construct an Effective Field Theory (EFT) which is defined on a NC spacetime with a canonical structure

$$[\hat{x}^\mu, \hat{x}^\nu] = i\theta^{\mu\nu} = i\frac{1}{\Lambda_{\text{NC}}^2}C^{\mu\nu} \quad (1)$$

and has—ignoring potential violations of the decoupling theorem engendered by UV/IR mixing in higher orders of perturbation theory—the Standard Model (SM) as low energy limit for $\sqrt{s} \ll \Lambda_{\text{NC}}$. While it is reasonably straightforward to construct a NC version of QED and there have been several studies of the phenomenological consequences of NCQED [4, 5], it is impossible to comprise the whole SM without additional constructions. The key issue here is the realization of gauge invariance on NC spaces [1, 6]. Early attempts suffered from the fact that only certain gauge groups could be realized (in particular $U(N)$, but not $SU(N)$) and from the quantization of $U(1)$ charges. The latter is caused by the Ward identity for the coupling of gauge fields to matter, which forces the triple gauge boson coupling to be identical to the coupling of *each* particle to the gauge bosons. Consequently, all particles must carry the *same* charge, which is incompatible with the hypercharge assignments in the SM (see however [7] for a clever symmetry breaking mechanism realizing the correct hypercharges at the price of introducing additional heavy gauge bosons).

A general way to overcome the aforementioned problems is provided by the Seiberg-Witten Map (SWM) [1]. It is an asymptotic expansion in the noncommutativity $\theta^{\mu\nu}$ which relates the fields on the NC spaces to the fields

on a commutative space. $SU(N)$ gauge groups and arbitrary $U(1)$ charges can be realized by going from Lie algebras to their enveloping algebras. The additional degrees of freedom introduced in this way can be eliminated by the freedom in the SWM [6]. In this approach, the rôle of the triple gauge boson couplings in the Ward identities is taken over by new contact terms and the problem with charge quantization does not appear. A realistic model including the full SM has been proposed soon after the introduction of the SWM [8]. Our goal in the current paper is to give a new example of a search for signals of NC structures in such a realistic model and also to present the methods needed for their calculation.

The organization of the current paper is as follows: in section 2 we give a brief introduction to the Noncommutative Standard Model (NCSM), in section 3 we demonstrate which new effects will appear in the NCSM and propose fermion pair production at a future photon collider as a process where to search for signals of NC theories. The formalism used in our analysis—helicity amplitudes with antisymmetric rank-two tensor fields—is presented in section 4. We then analyze the angular distribution in $\gamma\gamma \rightarrow f\bar{f}$. In section 5 we discuss consistency checks for our calculation. In section 6 we present our numerical results before concluding and giving a short outlook to some further possibilities in section 7. We add an extensive appendix with our conventions and details of the formalism used as well as a list of the Feynman rules, which will serve as a reference for future work [9].

2 The Noncommutative Standard Model

The NC structure of spacetime is associated with a scale Λ_{NC}

$$[\hat{x}^\mu, \hat{x}^\nu] = i\theta^{\mu\nu} = i\frac{1}{\Lambda_{\text{NC}}^2}C^{\mu\nu} = i\frac{1}{\Lambda_{\text{NC}}^2} \begin{pmatrix} 0 & -E^1 & -E^2 & -E^3 \\ E^1 & 0 & -B^3 & B^2 \\ E^2 & B^3 & 0 & -B^1 \\ E^3 & -B^2 & B^1 & 0 \end{pmatrix} \quad (1')$$

and the noncommutativity $\theta^{\mu\nu}$ is a real antisymmetric matrix, assumed here to be constant, which can be understood as a spurion breaking Lorentz invariance. The dimensionless “electric” and “magnetic” parameters \vec{E} and \vec{B} have been introduced in (1') for future convenience. The microscopic origin of the spurion $\theta^{\mu\nu}$ is irrelevant as long as we are merely studying the EFT, where it appears as a coefficient in front of operators of dimension six or higher.

Functions on NC manifolds are realized by functions on a commutative manifold, when their pointwise product is replaced by the Moyal-Weyl \star -

product:

$$\begin{aligned}
(f \star g)(x) &= \exp \left[\frac{i}{2} \theta^{\mu\nu} \frac{\partial}{\partial x^\mu} \frac{\partial}{\partial y^\nu} \right] f(x)g(y) \Big|_{y \rightarrow x} \\
&= f(x)g(x) + \frac{i}{2} \theta^{\mu\nu} (\partial_\mu f(x)) (\partial_\nu g(x)) + \mathcal{O}(\theta^2). \quad (2)
\end{aligned}$$

Gauge theories on a NC manifold can then be constructed with the help of the SWM, which expresses the NC matter and gauge fields $\hat{\Psi}$ and \hat{A}_μ as functions of commutative matter and gauge fields Ψ and A_μ so that the NC gauge transformations $\hat{\Psi} \rightarrow \hat{\Psi}'$ and $\hat{A} \rightarrow \hat{A}'$ are realized by the commutative gauge transformations $\Psi \rightarrow \Psi'$ and $A \rightarrow A'$

$$\hat{A}'(A) = \hat{A}(A') \quad (3a)$$

$$\hat{\Psi}'(\Psi, A) = \hat{\Psi}(\Psi', A'). \quad (3b)$$

To lowest order in $\theta^{\mu\nu}$, the SWMs are

$$\hat{\Psi} = \Psi + \frac{1}{2} \theta^{\mu\nu} A_\nu \partial_\mu \Psi + \frac{i}{8} \theta^{\mu\nu} [A_\mu, A_\nu] \Psi + \mathcal{O}(\theta^2) \quad (4a)$$

$$\hat{A}_\lambda = A_\lambda + \frac{1}{4} \theta^{\mu\nu} \{A_\nu, \partial_\mu A_\lambda\} + \frac{1}{4} \theta^{\mu\nu} \{F_{\mu\lambda}, A_\nu\} + \mathcal{O}(\theta^2). \quad (4b)$$

Equipped with this machinery, the construction of the NCSM is now straightforward: one has to replace each field by the corresponding SWM and all products by \star -products. This leads to the Lagrangian given in [8] from which the Feynman rules can be derived. The Feynman rules needed in the present paper are collected in appendix C.

The contributions of the higher-dimensional operators are suppressed by the ratios $\Lambda_{EW}^2/\Lambda_{NC}^2$ and s/Λ_{NC}^2 of the electroweak scale, the NC scale and the CMS energy of the process. There have already been several papers exploring the constraints from past and present-day experiments (at a moment mainly from the non-observation of the Lorentz-violating Z decays $Z \rightarrow \gamma\gamma, gg$ at LEP, as well as from astrophysics [10, 11, 12, 13, 14]). The bound on Λ_{NC} is still surprisingly low, of the order of 100 – 200 GeV. In a low lying string scenario one could expect values for such a scale as low as $\Lambda_{NC} \gtrsim 1$ TeV.

3 New effects and signals

Due to the presence of the higher-dimensional operators, there will be deviations of decay rates and production cross sections from the SM predictions. Existing SM vertices receive corrections with new Lorentz structures and

there are new vertices coupling more than one gauge boson to matter fields. The latter are required by the former in order to retain gauge invariance. In addition, there can also be new gauge boson interactions not allowed in the SM, most prominently triple neutral gauge boson vertices such as $\gamma\gamma\gamma$, $Z\gamma\gamma$, ZZZ , Zgg , γgg [12].

In general, taking the effects of the noncommutativity into account, amplitudes for physical processes are asymptotic expansions in $\theta^{\mu\nu}$. Squared matrix elements at $\mathcal{O}(\theta^2)$ are (the subscripts 1 and 2 denote the order in θ)

$$|A|^2 = |A^{\text{SM}}|^2 + (A^{\text{SM}})^* A_1^{\text{NC}} + (A_1^{\text{NC}})^* A^{\text{SM}} + |A_1^{\text{NC}}|^2 + (A^{\text{SM}})^* A_2^{\text{NC}} + (A_2^{\text{NC}})^* A^{\text{SM}}. \quad (5)$$

For processes forbidden in the SM, only the term $|A_1^{\text{NC}}|^2$ contributes at this order. If there is a nonvanishing SM amplitude, all interference terms have to be taken into account. Consequently, the term with the first order NC amplitude squared has to be dropped as long as we do not know the second order NC amplitudes, which depend on the second order terms in the SWM for the fields. Unfortunately, the SWMs for the NCSM are not yet known beyond first order. Therefore we concentrate in the present paper on the first order interference terms.

Our proposal is to consider fermion pair production $\gamma\gamma \rightarrow f\bar{f}$ at a future photon collider. Such a machine has been proposed for a future linear e^+e^- -collider with energies up to 1 TeV [15]. Highly energetic photons are produced with the help of Compton backscattering of laser photons off the LINAC electron beam. Thanks to the Compton scattering cross section, the photons can be delivered with a high degree of polarization. Indeed polarization will be available from day one, because it is required for obtaining a photon spectrum concentrated at high energies [16]. This will be crucial for our considerations.

The center of mass energy is planned to be in the range of several hundreds of GeV. We will assume massless fermions in our calculation and postpone the discussion of the specific features of top-quark production and decays to a future publication. Theoretically, the approximation of massless fermions together with the fact of having polarized photons suggests to use the very elegant formalism of helicity amplitudes [17, 18] for evaluating the cross section.

4 Helicity amplitudes with noncommutativity

The major addition to the established helicity amplitude machinery [17, 18] required by our application is the spinor representation of antisymmetric rank-two tensor fields in order to incorporate the noncommutativity into the spinor products. With the help of the Schouten identity (21) the noncommutativity can be converted in a very elegant way to a spinor expression containing only the spinor metric and a symmetric rank-2 spinor (for a textbook presentation cf. [19]):

$$\theta_{AA',BB'} = \theta^{\mu\nu} \bar{\sigma}_{\mu,AA'} \bar{\sigma}_{\nu,BB'} = \phi_{AB} \epsilon_{A'B'} + \bar{\phi}_{A'B'} \epsilon_{AB} \quad (6)$$

with $(\phi_{AB})^* = \bar{\phi}_{A'B'}$. Then $\phi_{AB} = \frac{1}{2} \theta_{A\dot{C},B\dot{C}}$ is symmetric with three independent complex components

$$\phi_{11} = -E_- - iB_- \quad (7a)$$

$$\phi_{12} = E_3 + iB_3 = \phi_{21} \quad (7b)$$

$$\phi_{22} = E_+ + iB_+, \quad (7c)$$

using the parameterization (1'), with $E_{\pm} = E^1 \pm iE^2$, $B_{\pm} = B^1 \pm iB^2$. With the help of this expression, all amplitudes can be expressed as contractions of Weyl-van der Waerden spinors with ϕ and among themselves.

To convert contractions of the noncommutativity with two vectors (momenta and polarization vectors)

$$(V_1 \theta V_2) := V_{1,\mu} \theta^{\mu\nu} V_{2,\nu} = V_1^0 (\vec{E} \cdot \vec{V}_2) - V_2^0 (\vec{E} \cdot \vec{V}_1) - \vec{B} \cdot (\vec{V}_1 \times \vec{V}_2) \quad (8)$$

into spinor expressions

$$(V_1 \theta V_2) = \frac{1}{2} \text{Re} [\langle v_1 v_2 \rangle^* \langle v_1 \phi v_2 \rangle]$$

we introduce the symmetric spinor products

$$\langle p \phi q \rangle = p^A \phi_{AB} q^B = \langle q \phi p \rangle, \quad \langle p \phi q \rangle^* = p^{\dot{A}} \bar{\phi}_{\dot{A}\dot{B}} q^{\dot{B}}. \quad (9)$$

As this is a non-standard spinor product we give an explicit expression (in the conventions described in appendix A)

$$\begin{aligned} \langle p \phi q \rangle &= \epsilon^{BA} p_A \phi_{BC} \epsilon^{CD} q_D = -p_A \epsilon^{AB} \phi_{BC} \epsilon^{CD} q_D \\ &= \phi_{11} p_2 q_2 + \phi_{22} p_1 q_1 - \phi_{12} (p_1 q_2 + p_2 q_1). \end{aligned} \quad (10)$$

We study the processes $\gamma(k_1)\gamma(k_2) \rightarrow f(p_1)\bar{f}(p_2)$. In the SM, there are t - and u -channel exchange diagrams

$$A_t^{\text{SM}} = \text{[t-channel SM diagram]} \quad A_u^{\text{SM}} = \text{[u-channel SM diagram]} \quad . \quad (11)$$

Due to helicity conservation, the only nonvanishing combinations for massless fermions in the final state are $(\pm, \mp) \rightarrow (\pm, \mp)$ and $(\pm, \mp) \rightarrow (\mp, \pm)$. Since we are interested in the interference of the NCSM with the SM amplitude, we do not have to calculate the NC amplitude for the other combinations.

There are two $O(\theta)$ contributions for each standard model diagram¹

$$A_{t,1}^{\text{NC}} = \text{[t-channel NC diagram 1]} \quad A_{t,2}^{\text{NC}} = \text{[t-channel NC diagram 2]} \quad (12a)$$

$$A_{u,1}^{\text{NC}} = \text{[u-channel NC diagram 1]} \quad A_{u,2}^{\text{NC}} = \text{[u-channel NC diagram 2]} \quad . \quad (12b)$$

The contact term is required by gauge invariance

$$A_c^{\text{NC}} = \text{[contact term diagram]} \quad , \quad (12c)$$

and there are two additional s -channel diagrams that depend on new coupling constants $K_{\gamma\gamma\gamma}$ and $K_{Z\gamma\gamma}$ ²

$$A_{s,\gamma}^{\text{NC}} = \text{[s-channel NC diagram 1]} \quad A_{s,Z}^{\text{NC}} = \text{[s-channel NC diagram 2]} \quad . \quad (12d)$$

¹The Feynman rules are collected in appendix C

²Matching the NCSM to the SM constrains the new triple gauge boson couplings, but the two couplings can not vanish simultaneously [12].

The explicit expressions for the helicity amplitudes for the choice $g_- = p_1$ and $g_+ = p_2$ of gauge spinors are

$$A_{s,Z}^{\text{NC},(+,-)} + A_{s,\gamma}^{\text{NC},(+,-)} = K_{\gamma Z}^{(+,-)} \left[c_1 \cdot \langle p_1 k_1 \rangle^* \langle p_2 k_1 \rangle + c_2 \cdot \frac{\langle p_1 p_2 \rangle^* \langle p_2 k_1 \rangle}{\langle p_2 k_1 \rangle^*} + c_3 \cdot \frac{\langle p_1 k_2 \rangle^* \langle p_2 p_1 \rangle}{\langle p_1 k_2 \rangle} \right] \quad (13a)$$

$$A_{s,Z}^{\text{NC},(-,+)} + A_{s,\gamma}^{\text{NC},(-,+)} = K_{\gamma Z}^{(-,+)} \cdot c_1 \cdot \langle p_2 k_1 \rangle^* \langle p_1 k_1 \rangle \quad (13b)$$

with the coefficients

$$c_1 = 2(k_1 \theta k_2)(\varepsilon_1 \varepsilon_2) - s(\varepsilon_1 \theta \varepsilon_2) \quad (14a)$$

$$c_2 = \sqrt{2}[(k_1 \theta \varepsilon_2)s - 2(k_1 \theta k_2)(\varepsilon_2 k_1)] \quad (14b)$$

$$c_3 = \sqrt{2}[(k_2 \theta \varepsilon_1)s + 2(k_1 \theta k_2)(\varepsilon_1 k_2)] \quad (14c)$$

and propagator factors

$$C_{\gamma\gamma} = \frac{2e^2 Q_f \sin(2\theta_W) K_{\gamma\gamma\gamma}}{s} \quad (15a)$$

$$K_{\gamma Z}^{(+,-)} = C_{\gamma\gamma} + \frac{4g^2 s_W^4 Q_f K_{Z\gamma\gamma}}{s - M_Z^2 + iM_Z \Gamma_Z} \quad (15b)$$

$$K_{\gamma Z}^{(-,+)} = C_{\gamma\gamma} - \frac{4g^2 s_W^2 K_{Z\gamma\gamma}}{s - M_Z^2 + iM_Z \Gamma_Z} (T^3 - s_W^2 Q_f) . \quad (15c)$$

The remaining diagrams contribute

$$A_{t,1}^{(+,-)} = \frac{-e^2 Q_f^2 \langle p_1 k_1 \rangle \langle p_2 p_1 \rangle \langle p_1 k_2 \rangle^*}{\sqrt{2}t \langle p_1 k_2 \rangle} \times \left[(\varepsilon_1 \theta p_1) \langle p_1 k_1 \rangle^* - \sqrt{2}(k_1 \theta p_1) \frac{\langle p_1 p_2 \rangle^*}{\langle p_2 k_1 \rangle^*} \right] \quad (16a)$$

$$A_{t,1}^{(-,+)} = \frac{-e^2 Q_f^2 \langle p_1 k_1 \rangle \langle p_2 k_2 \rangle^* \langle p_1 k_1 \rangle}{t \langle p_1 k_2 \rangle} (k_1 \theta p_1) \quad (16b)$$

$$A_{u,1}^{(+,-)} = \frac{-e^2 Q_f^2 \langle k_1 p_2 \rangle \langle p_1 k_2 \rangle^*}{\sqrt{2}u \langle p_2 k_1 \rangle^*} \left[(\varepsilon_2 \theta p_1) \langle k_2 p_1 \rangle \langle p_1 p_2 \rangle^* + \sqrt{2}(k_2 \theta p_1) \langle k_2 p_2 \rangle^* \right] \quad (16c)$$

$$A_{u,1}^{(-,+)} = 0 \quad (16d)$$

$$A_{t,2}^{(+,-)} = \frac{-e^2 Q_f^2 \langle p_1 k_2 \rangle^* \langle p_1 p_2 \rangle^* \langle p_1 k_1 \rangle}{\sqrt{2}t \langle p_2 k_1 \rangle^*} \left[(\varepsilon_2 \theta p_2) \langle k_2 p_2 \rangle - \sqrt{2}(k_2 \theta p_2) \frac{\langle p_1 p_2 \rangle}{\langle p_1 k_2 \rangle} \right] \quad (16e)$$

$$A_{t,2}^{(-,+)} = \frac{-e^2 Q_f^2}{t} \frac{\langle k_1 p_1 \rangle \langle p_2 k_2 \rangle^* \langle k_2 p_2 \rangle^*}{\langle p_2 k_1 \rangle^*} (k_2 \theta p_2) \quad (16f)$$

$$A_{u,2}^{(+,-)} = \frac{-e^2 Q_f^2}{\sqrt{2}u} \frac{\langle k_1 p_2 \rangle \langle p_1 k_2 \rangle^*}{\langle p_1 k_2 \rangle} \left[(\epsilon_1 \theta p_2) \langle p_1 p_2 \rangle \langle p_2 k_1 \rangle^* - \sqrt{2} (k_1 \theta p_2) \langle p_1 k_1 \rangle \right] \quad (16g)$$

$$A_{u,2}^{(-,+)} = 0 \quad (16h)$$

$$A_c^{(+,-)} = \frac{e^2 Q_f^2}{2} \left[(\epsilon_1 \theta \epsilon_2) (\langle p_1 k_1 \rangle^* \langle p_2 k_1 \rangle - \langle p_1 k_2 \rangle^* \langle p_2 k_2 \rangle) \right. \\ \left. + \sqrt{2} ((k_1 - k_2) \theta \epsilon_1) \frac{\langle p_1 k_2 \rangle^* \langle p_2 p_1 \rangle}{\langle p_1 k_2 \rangle} \right. \\ \left. - \sqrt{2} ((k_1 - k_2) \theta \epsilon_2) \frac{\langle p_1 p_2 \rangle^* \langle p_2 k_1 \rangle}{\langle p_2 k_1 \rangle^*} \right] \quad (16i)$$

$$A_c^{(-,+)} = \frac{e^2 Q_f^2}{2} (\epsilon_1 \theta \epsilon_2) \left[\langle p_2 k_1 \rangle^* \langle p_1 k_1 \rangle - \langle p_2 k_2 \rangle^* \langle p_1 k_2 \rangle \right]. \quad (16j)$$

The amplitudes with the other combination of photon helicities can be obtained by simply interchanging k_1 with k_2 . The well known SM amplitudes have been reproduced in appendix D.

From the analytical form, one can deduce that the interference depends only on the space-time non-commutativity \vec{E} , but not on the space-space noncommutativity \vec{B} . In fact, a nonvanishing interference appears only for non-zero E^1 or E^2 . Note that this dependence on the components of $\theta^{\mu\nu}$ in the NCSM is different from NCQED [5].

In figure 1, the differential cross section at a center-of-mass energy of 800 GeV is plotted against the azimuthal angle ϕ . One sees that the integration over the full solid angle will yield the same result for the interference as for the SM cross section, because the squared matrix element is proportional to $\sin(\phi + \phi_0)$, where ϕ_0 is a phase which depends on the spatial orientation of the noncommutativity.

In the same way as it is possible for a Z in the NCSM to decay into two photons violating the Yang-Landau theorem, it can be produced resonantly in photon collisions. Figure 2 shows the shapes of the interference contributions near the Z resonance for different values of the azimuthal angle. The effect for $\phi = 0$ is only due to the imaginary part of the SM amplitude close to the resonance and is therefore absent in figure 1, where $\sqrt{s} \gg M_Z$. Unfortunately, this resonance will hardly be visible for $\Lambda_{\text{NC}} \gg M_Z$.

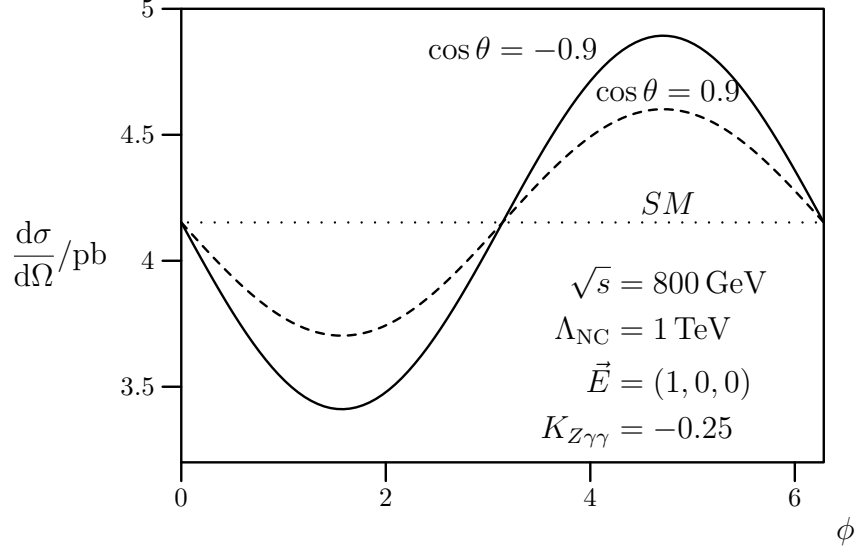


Figure 1: Dependence of the differential NCSM cross section on the azimuthal angle ϕ for the time-like noncommutativity \vec{E} perpendicular to the beam axis.

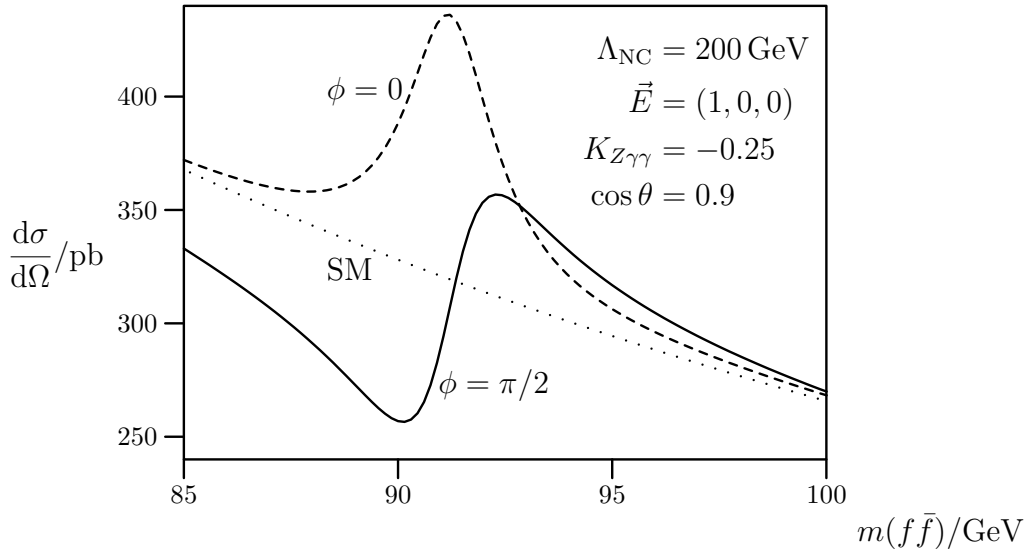


Figure 2: The interference of the SM and $\mathcal{O}(\theta)$ NCSM amplitudes around the Z resonance is plotted for different values of the azimuthal angle ϕ .

5 Consistency Checks: Amplitudes and Ward Identity

In order to control the numerical stability of a simulation as well as to assure the correctness of our results, we have performed several cross checks. Our first check was to compare numerically the amplitude calculated between two completely different formalisms: helicity amplitudes on the one hand and Dirac spinors and polarization vectors on the other hand³. We found the results to agree within numerical accuracy.

Another way to check the resulting amplitude is to prove that the Ward identity is fulfilled. Writing the Dirac matrix strings for the amplitudes

$$iA_{\mu_2\mu_1}^t = \bar{u}(p_1) \left[ig\gamma_{\mu_2} \frac{i}{\not{p}_1 + \not{k}_2} ig\Gamma_{\mu_1}(k_1, p_2) + ig\Gamma_{\mu_2}(k_2, k_1 + p_2) \frac{i}{\not{p}_1 + \not{k}_2} ig\gamma_{\mu_1} \right] v(p_2) \quad (17a)$$

$$iA_{\mu_2\mu_1}^u = \bar{u}(p_1) \left[ig\gamma_{\mu_1} \frac{i}{\not{p}_1 + \not{k}_1} ig\Gamma_{\mu_2}(k_2, p_2) + ig\Gamma_{\mu_1}(k_1, k_2 + p_2) \frac{i}{\not{p}_1 + \not{k}_1} ig\gamma_{\mu_2} \right] v(p_2) \quad (17b)$$

$$iA_{\mu_2\mu_1}^c = \bar{u}(p_1) ig^2 H_{\mu_2\mu_1}(k_2, k_1) v(p_2) \quad (17c)$$

and using (cf. appendix C)

$$k^\mu \Gamma_\mu(k, p) = 0 \quad (18a)$$

$$\varepsilon^\mu \Gamma_\mu(k, p) = \frac{i}{2} [(k\theta p)\not{\varepsilon} - (k\theta\varepsilon)\not{p} - (\varepsilon\theta p)\not{k}] \quad (18b)$$

$$\begin{aligned} k_1^{\mu_1} \varepsilon_2^{\mu_2} H_{\mu_1\mu_2}(k_1, k_2) &= \frac{i}{2} [(k_1\theta k_2)\not{\varepsilon}_2 - (\varepsilon_2\theta k_2)\not{k}_1 - (k_1\theta\varepsilon_2)\not{k}_2] \\ &= \varepsilon_2^{\mu_2} \Gamma_{\mu_2}(k_1, k_2) = -\varepsilon_2^{\mu_2} \Gamma_{\mu_2}(k_2, k_1), \end{aligned} \quad (18c)$$

one sees analytically that the Ward identity is satisfied indeed:

$$\begin{aligned} k_2^{\mu_2} \varepsilon_1^{\mu_1} (A_{\mu_2\mu_1}^t + A_{\mu_2\mu_1}^u + A_{\mu_2\mu_1}^c) &= \\ g^2 \bar{u}(p_1) [-\varepsilon_1^{\mu_1} \Gamma_{\mu_1}(k_1, p_2) + \varepsilon_1^{\mu_1} \Gamma_{\mu_1}(k_1, k_2 + p_2) - \varepsilon_1^{\mu_1} \Gamma_{\mu_1}(k_1, k_2)] v(p_2) &= 0. \end{aligned} \quad (19)$$

The gauge independence manifests itself in the independence of the helicity amplitudes from the choice of the gauge spinor. We have verified this independence for our results within the numerical accuracy.

³Using an extension of the optimizing matrix element compiler `O'Mega` [20].

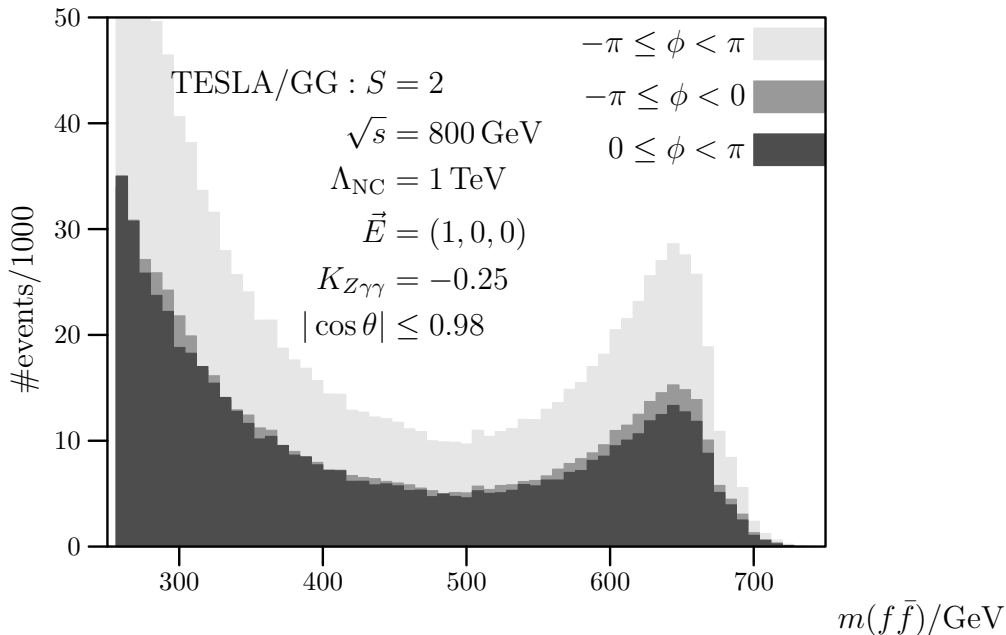


Figure 3: Number of events per year in the two halfspheres $\phi < 0$ and $\phi > 0$ for $\sqrt{s} = 800 \text{ GeV}$.

6 Results: Cross Section and Event Generation

To get a realistic cross section from the squared matrix element, one has to fold the resulting cross section with the photon spectrum produced in Compton scattering for the photon collider. For this purpose, the program `Circe 2.0` has been used [21], which parameterizes the results of a microscopic simulation of the beam dynamics [22].

As already mentioned in section 3, the integrated cross section at order θ does not differ from the SM cross section since it is linear in trigonometric functions of the azimuthal angle. However, in the polarized cross section it is possible to scan over the final state fermions to look for angular dependent deviations from the SM prediction.

In figure 3 we show the number of binned events over the invariant mass of the fermion pair, assuming integrated luminosities of 400 fb^{-1} for 200 GeV, 1000 fb^{-1} for 500 GeV and 2000 fb^{-1} for 1 TeV. These are expected [15] for one year of running with 30% uptime. For the $Z\gamma\gamma$ couplings we chose the central value $K_{Z\gamma\gamma} = -0.25$, but the cross section and the angular variation away from the Z resonance do not depend very much on this choice. A cut

of about 11.5 degrees around each beam axis has been applied.

Here one should notice one important point: A non-zero signal can only be seen in the case that the helicities of the two photons are different, so that they add up to a total helicity of two. Therefore, the photon collider has to be run in the d -wave mode ($S = 2$) with different helicities. Originally, the photon collider was proposed to be run in the s -wave mode ($S = 0$) which is mandatory in the study of the quantum numbers of scalar or pseudoscalar particles like the Higgs. Fortunately, the photon collider can be operated in each of the two modes and one can easily switch between them.

In order to estimate the maximum effect we have assumed that the axis of alignment for the detector relative to the noncommutativity is known and have subdivided the full solid angle accordingly. In practice, one first has to scan through the angular distributions of the fermions in order to find deviations from the isotropic distribution around the beam axis. Then, one can maximize the anisotropy and in such a way fit the angular distribution to the data. In this process one has to take into account the fact that, due to the rotation of the earth and the rotation of the earth around the sun, the direction of the noncommutativity relative to the collider and the detector is almost certainly not constant. Instead one must use a coordinate system fixed in space. Since the orientation of the noncommutativity can therefore not be optimized for a maximal effect, the results shown in figures 3-5 are an optimistic upper limit and should be expected to be diluted by a factor of two in addition to the usual systematic uncertainties.

Figures 3-5 show that a signal can be seen easily if the scale Λ_{NC} is not far below the CMS-mass energy \sqrt{s} of the linear collider, but generically the result gets worse if the scale is lower. Our present calculation must not be used for collider energies higher than the scale Λ_{NC} , since higher orders in θ can only be neglected if $s/(\Lambda_{\text{NC}})^2 \lesssim 1$.

Other useful processes in the search for a signal of the NCSM are $\gamma\gamma \rightarrow \gamma\gamma$, $\gamma\gamma \rightarrow \gamma Z$ and $\gamma\gamma \rightarrow ZZ$. However, the dimension-six operators consisting of three field strength tensors engendered by the kinetic terms in the NCSM cannot contain four neutral electroweak gauge bosons, because $SU(2)$ has rank one. Therefore interferences with such (loop-induced) SM amplitudes occur only at order θ^2 .

7 Conclusions

An extension of the Standard Model to noncommutative spacetime—which arises in certain low-energy limits of string theories—offers a variety of new phenomena. Due to the presence of an antisymmetric rank-two spurion field

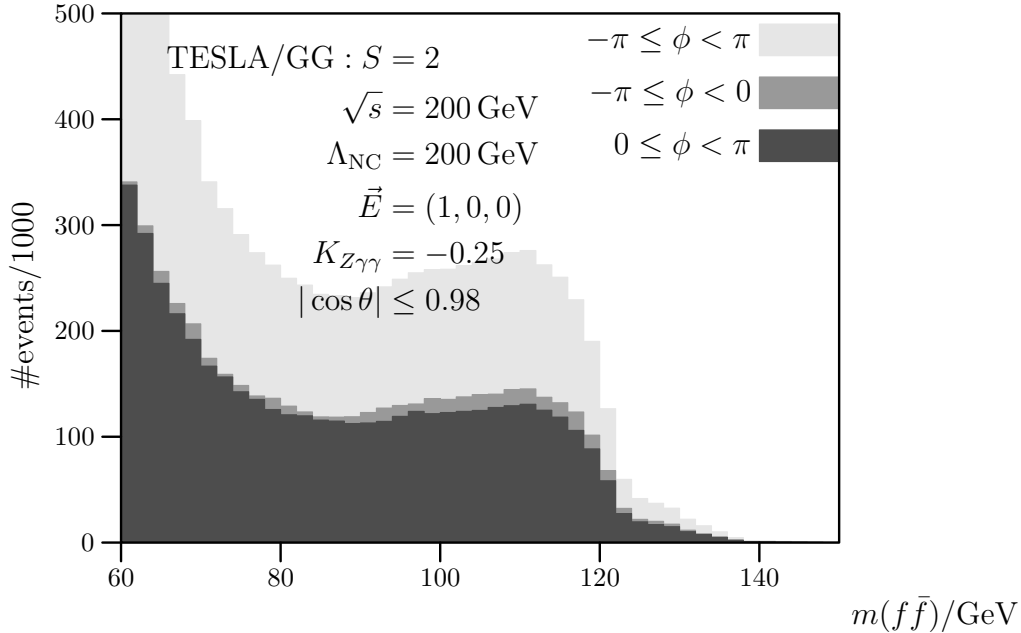


Figure 4: Number of events per year in the two halvespheres $\phi < 0$ and $\phi > 0$ for $\sqrt{s} = 200$ GeV.

which breaks Lorentz invariance at a scale Λ_{NC} the SM is supplemented by a number of dimension-six operators which result in deviations of decay rates, production cross sections and other observables from their SM predictions. In this paper we have focused on fermion pair production at a future photon collider as an example for exploring the sensitivity of future accelerator experiments to the free parameters $\theta^{\mu\nu}$, $K_{Z\gamma\gamma}$, etc. of such models.

A generic signal for noncommutativity is the violation of angular momentum conservation, which stems from the noncommutativity acting as a static source of angular momentum and which leads to violations of the isotropic distribution of final state particles around the beam axis.

Polarization is a helpful—if not mandatory—ingredient of searches for signals of noncommutative theories. Therefore, the high degree of polarization for the electron (and possibly also for the positron) beam at the future linear collider facilitates searches for the NCSM directly at the lepton collider [9]. The methods presented here will be used in the corresponding calculations. Nevertheless, the very low background environment of photon collisions provides a good example for NCSM searches. In a conservative estimate, a photon collider will be sensitive to scales of the order of $\Lambda_{\text{NC}} \sim 1$ TeV, but once enough data will be available, experimental ingenuity will certainly push

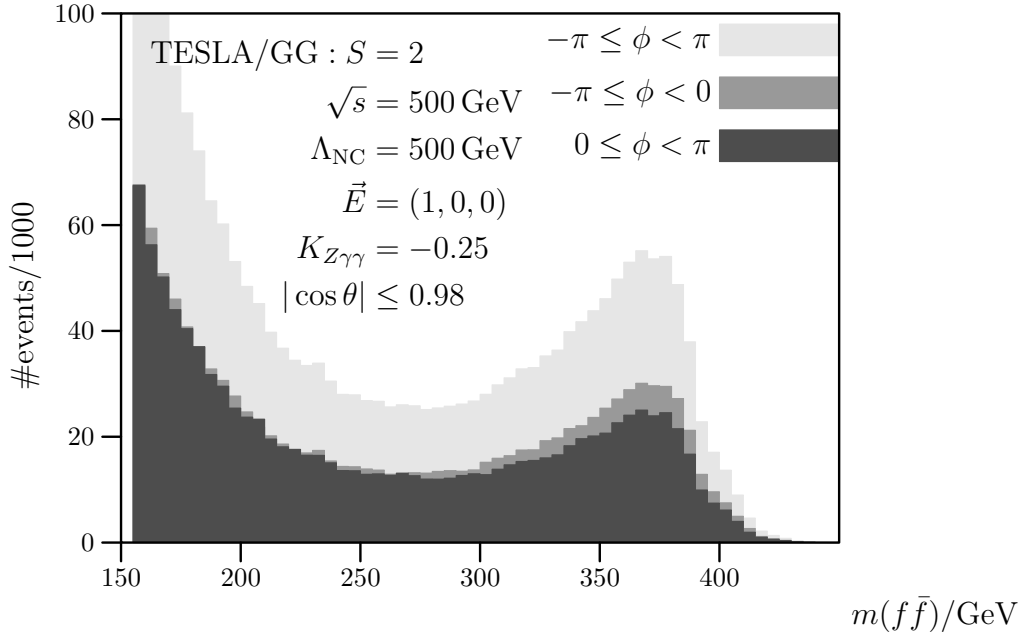


Figure 5: Number of events per year in the two halfspheres $\phi < 0$ and $\phi > 0$ for $\sqrt{s} = 500$ GeV.

this limit upwards.

Acknowledgments

T. O. is supported by the Deutsche Forschungsgemeinschaft (DFG), grant RU 311/1-1, and the Bundesministerium für Bildung und Forschung Germany, grant 05HT1RDA/6. J. R. is supported by the DFG Sonderforschungsbereich (SFB) “Transregio 9 – Computergestützte Theoretische Teilchenphysik” and the Graduiertenkolleg (GK) “Hochenergiephysik und Teilchenastrophysik”.

We are grateful to Ana Alboteanu and Klaus Mönig for valuable discussions.

A Spinors and Spinor Products

A.1 General conventions

Complex conjugation interchanges dotted and undotted indices: $\bar{\xi}_{\dot{A}} = (\xi_A)^*$, $\xi^A = (\bar{\xi}^{\dot{A}})^*$. The spinor metric is $\epsilon^{AB} = \epsilon^{\dot{A}\dot{B}} = \epsilon_{AB} = \epsilon_{\dot{A}\dot{B}}$ with $\epsilon_{AB} = -\epsilon_{BA}$

and $\epsilon_{12} = +1$. Our convention for lowering or raising of spinor indices is

$$\begin{aligned}\xi^A &= \epsilon^{AB}\xi_B, & \bar{\xi}^{\dot{A}} &= \epsilon^{\dot{A}\dot{B}}\bar{\xi}_{\dot{B}}, \\ \xi_A &= \xi^B\epsilon_{BA}, & \bar{\xi}_{\dot{A}} &= \bar{\xi}^{\dot{B}}\epsilon_{\dot{B}\dot{A}}.\end{aligned}\tag{20}$$

The antisymmetric spinor product for commuting components $\eta\xi = \eta_A\xi^A = \eta_1\xi_2 - \eta_2\xi_1$, $\bar{\eta}\bar{\xi} = \bar{\eta}_{\dot{A}}\bar{\xi}^{\dot{A}} = (\eta_1\xi_2 - \eta_2\xi_1)^* = \bar{\eta}_{\dot{1}}\bar{\xi}_{\dot{2}} - \bar{\eta}_{\dot{2}}\bar{\xi}_{\dot{1}}$ and therefore $(\eta\xi)^* = (\bar{\eta}\bar{\xi})$, $\eta\xi = -\bar{\eta}\bar{\xi}$, $\bar{\eta}\bar{\xi} = -\xi\bar{\eta}$, and $\xi\xi = \bar{\xi}\bar{\xi} = 0$. ‘‘Tilting’’ of indices: $\eta_A\xi^A = \eta^B\epsilon_{BA}\epsilon^{AC}\xi_C = \eta^B(-\delta_B^C)\xi_C = -\eta^A\xi_A$ and the Schouten identity is

$$\epsilon^{AB}\epsilon^{CD} + \epsilon^{AC}\epsilon^{DB} + \epsilon^{AD}\epsilon^{BC} = 0.\tag{21}$$

The vector of the Pauli matrices is defined by $\sigma^{\mu,\dot{A}B} = (\mathbf{1}, \vec{\sigma})$ and $\bar{\sigma}_{\dot{A}B}^\mu = (\mathbf{1}, -\vec{\sigma})$. We always distinguish the position of the index:

$$\sigma^1 = -\sigma_1 = \begin{pmatrix} 0 & 1 \\ 1 & 0 \end{pmatrix}, \quad \sigma^2 = -\sigma_2 = \begin{pmatrix} 0 & -i \\ i & 0 \end{pmatrix}, \quad \sigma^3 = -\sigma_3 = \begin{pmatrix} 1 & 0 \\ 0 & -1 \end{pmatrix}.\tag{22}$$

We conclude with some formulae for the spin tensors that fix our conventions and makes the derivation of the spinor representations more transparent. Hermiticity $\sigma^{\mu,\dot{A}B} = \sigma^{\mu,B\dot{A}}$, $\bar{\sigma}_{\dot{A}B}^\mu = \bar{\sigma}_{B\dot{A}}^\mu$; complex conjugation $\sigma_{\dot{A}B}^\mu = (\bar{\sigma}_{\dot{A}B}^\mu)^* = (\mathbf{1}, -\vec{\sigma}^*) = (\mathbf{1}, -\sigma^1, \sigma^2, -\sigma^3)$, lowering indices $\sigma_{\dot{A}B}^\mu = \sigma^{\mu,\dot{C}D}\epsilon_{\dot{C}\dot{A}}\epsilon_{DB} = (\mathbf{1}, -\sigma^1, \sigma^2, -\sigma^3)$ (using $\sigma_{11}^\mu = \sigma^{\mu,\dot{2}2}$, $\sigma_{22}^\mu = \sigma^{\mu,\dot{1}1}$, $\sigma_{12}^\mu = -\sigma^{\mu,\dot{2}1}$, $\sigma_{21}^\mu = -\sigma^{\mu,\dot{1}2}$) and finally $\sigma_{\mu,\dot{A}B} = g_{\mu\nu}\sigma_{\dot{A}B}^\nu = (\mathbf{1}, \vec{\sigma}^*)$.

A.2 Decomposition of lightlike vectors

Contraction of a Minkowskian 4-vector with the spin tensor results in a spinor of rank two which is represented by a 2×2 Hermitian matrix for real vectors

$$K_{\dot{A}B} := k^\mu\sigma_{\mu,\dot{A}B} = k^\mu g_{\mu\nu}\sigma_{\dot{A}B}^\nu = k^0\mathbf{1} - \vec{k}(-\vec{\sigma})^* = \begin{pmatrix} k^0 + k^3 & k^1 + ik^2 \\ k^1 - ik^2 & k^0 - k^3 \end{pmatrix},\tag{23}$$

which allows to write 4-vector products as spinor products

$$2k \cdot p = k_\mu 2g^{\mu\nu}p_\nu = k_\mu\sigma_{\dot{A}B}^\mu\sigma^{\nu,\dot{A}B}p_\nu = K_{\dot{A}B}P^{\dot{A}B}.\tag{24}$$

For lightlike momenta, the momentum spinor matrix can be written as a tensor product

$$K_{\dot{A}B} = k_{\dot{A}}k_B, \quad k_{\dot{A}} = (k_A)^*, \quad \text{with } k_A = \left(\frac{(p^1 - ip^2)/\sqrt{p^0 - p^3}}{\sqrt{p^0 - p^3}} \right),\tag{25}$$

so that the spinor product is [17, 18]

$$\langle pq \rangle = (p_1 - ip_2) \frac{\sqrt{q_0 - q_3}}{\sqrt{p_0 - p_3}} - (q_1 - iq_2) \frac{\sqrt{p_0 - p_3}}{\sqrt{q_0 - q_3}}, \quad (26)$$

and we find

$$|\langle pq \rangle|^2 = 2p \cdot q. \quad (27)$$

B Constants, Expressions and Abbreviations

Here we summarize expressions containing the noncommutativity and polarization vectors:

$$(p\theta\varepsilon_+(k)) = \frac{\langle p\phi g_+ \rangle^* \langle pk \rangle + \langle p\phi k \rangle \langle pg_+ \rangle^*}{2\sqrt{2} \langle g_+ k \rangle^*} \quad (28a)$$

$$(p\theta\varepsilon_-(k)) = \frac{\langle p\phi k \rangle^* \langle pg_- \rangle + \langle p\phi g_- \rangle \langle pk \rangle^*}{2\sqrt{2} \langle g_- k \rangle}. \quad (28b)$$

If the momentum is that of the photon, the gauge spinor cancels out,

$$(k\theta\varepsilon_+(k)) = -\frac{1}{2\sqrt{2}} \langle k\phi k \rangle, \quad (k\theta\varepsilon_-(k)) = -\frac{1}{2\sqrt{2}} \langle k\phi k \rangle^*. \quad (29)$$

For the (+, -) polarization of the photons we have

$$(\varepsilon_+(k_1)\theta\varepsilon_-(k_2)) = \frac{\langle g_+ k_2 \rangle^* \langle k_1 \phi g_- \rangle + \langle k_1 g_- \rangle \langle g_+ \phi k_2 \rangle^*}{2 \langle g_+ k_1 \rangle^* \langle g_- k_2 \rangle}. \quad (30)$$

Translating vector to spinor expressions

$$(\varepsilon_1\varepsilon_2) = \frac{\langle g_+ k_2 \rangle^* \langle k_1 g_- \rangle}{\langle g_+ k_1 \rangle^* \langle g_- k_2 \rangle} \quad (31a)$$

$$(k_1\varepsilon_2) = \frac{1}{\sqrt{2}} \frac{\langle k_1 k_2 \rangle^* \langle k_1 g_- \rangle}{\langle g_- k_2 \rangle} \quad (31b)$$

$$(k_2\varepsilon_1) = \frac{1}{\sqrt{2}} \frac{\langle k_2 g_+ \rangle^* \langle k_2 k_1 \rangle}{\langle g_+ k_1 \rangle^*}. \quad (31c)$$

C The Feynman rules

In the Feynman rules for helicity amplitudes, external fermions are represented by

$$\Psi_+ = \begin{pmatrix} k_A \\ 0 \end{pmatrix}, \quad \Psi_- = \begin{pmatrix} 0 \\ k_{\dot{A}} \end{pmatrix}, \quad \bar{\Psi}_+ = (0, k_{\dot{A}}), \quad \bar{\Psi}_- = (k^A, 0). \quad (32)$$

The bispinor for an incoming antifermion is the same as the outgoing fermion with the interchange $+\leftrightarrow-$. (The outgoing antifermion's bispinor is related to the incoming fermion's bispinor in the same way). Polarization vectors of incoming photons:

$$\varepsilon_{+,\dot{A}B}(k) = \frac{\sqrt{2}g_{+,\dot{A}}k_B}{\langle g_+k \rangle^*}, \quad \varepsilon_{-,\dot{A}B}(k) = \frac{\sqrt{2}k_{\dot{A}}g_{-,B}}{\langle g_-k \rangle}. \quad (33)$$

Fermion and Z propagators in unitarity gauge:

$$f\bar{f} : \frac{i}{k^2} \begin{pmatrix} 0 & K_{\dot{A}\dot{B}} \\ K^{\dot{A}\dot{B}} & 0 \end{pmatrix}, \quad Z_\mu Z_\nu : \frac{-2i\epsilon_{\dot{A}\dot{C}}\epsilon^{BD}}{k^2 - M_Z^2 + iM_Z\Gamma_Z}. \quad (34)$$

A γ matrix coupling is translated to helicity amplitudes via

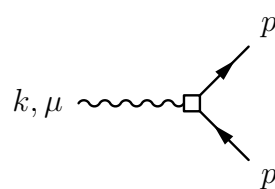
$$\gamma_\mu \left(C_L \frac{1-\gamma^5}{2} + C_R \frac{1+\gamma^5}{2} \right) \rightarrow \begin{pmatrix} 0 & C_L \delta_{\dot{B}}^{\dot{C}} \delta_A^D \\ C_R \epsilon^{\dot{A}\dot{C}} \epsilon^{BD} & 0 \end{pmatrix} \quad (35)$$

where $\dot{C}D$ are the spinor components of the vector degree of freedom and A, B the fermion spinor indices.

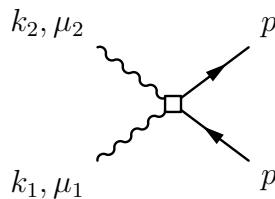
The Feynman rules of the NCSM can be read off from [8]. In order to simplify our formulae we introduce partial contractions

$$(k\theta)^\nu = k_\mu \theta^{\mu\nu}, \quad (\theta k)^\mu = \theta^{\mu\nu} k_\nu, \quad (k\theta)^\mu = -(\theta k)^\mu. \quad (36)$$

Vertices with *all momenta outgoing*



$$= ig(\gamma_\mu + \Gamma_\mu(k, p)) \quad (37a)$$



$$= ig^2 H_{\mu_1\mu_2}(k_1, k_2) \quad (37b)$$

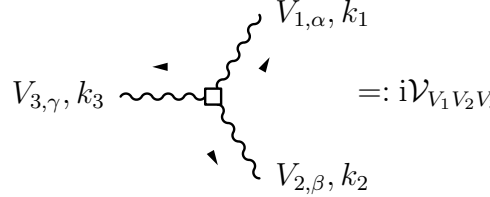
with

$$\Gamma_\mu(k, p) = \frac{i}{2} [(k\theta p)\gamma_\mu - (k\theta)_\mu \not{p} - (\theta p)_\mu \not{k}] = -\Gamma_\mu(p, k) \quad (38a)$$

$$H_{\mu_1\mu_2}(k_1, k_2) = \frac{i}{2} [\theta_{\mu_1\mu_2}(\not{k}_1 - \not{k}_2) + ((k_1 - k_2)\theta)_{\mu_1} \gamma_{\mu_2} - ((k_1 - k_2)\theta)_{\mu_2} \gamma_{\mu_1}]$$

$$= H_{\mu_2\mu_1}(k_2, k_1). \quad (38b)$$

And



$$=: i\mathcal{V}_{V_1 V_2 V_3} \quad (39)$$

with

$$\begin{aligned} V_{\alpha\beta\gamma}(k_1, k_2, k_3) = & \theta_{\alpha\beta} [(k_1 k_3) k_{2,\gamma} - (k_2 k_3) k_{1,\gamma}] \\ & + (k_1 \theta)_\alpha [k_{2,\gamma} k_{3,\beta} - (k_2 k_3) g_{\beta\gamma}] \\ & + (k_1 \theta k_2) [k_{3,\alpha} \eta_{\beta\gamma} - \eta_{\alpha\gamma} k_{3,\beta}] \\ & + \text{cyclical permutations of } \{(\alpha, k_1), (\beta, k_2), (\gamma, k_3)\}, \end{aligned} \quad (40)$$

the $\gamma_\alpha(k_1)\gamma_\beta(k_2)Z_\gamma(p)$ and $\gamma_\alpha(k_1)\gamma_\beta(k_2)\gamma_\gamma(k_3)$ vertices are given by

$$i\mathcal{V}_{Z\gamma\gamma} = +2e \sin(2\theta_W) K_{Z\gamma\gamma} \cdot V_{\alpha\beta\gamma}(k_1, k_2, p) \quad (41)$$

$$i\mathcal{V}_{\gamma\gamma\gamma} = -2e \sin(2\theta_W) K_{\gamma\gamma\gamma} \cdot V_{\alpha\beta\gamma}(k_1, k_2, k_3) \quad (42)$$

The coupling constants are related to the electroweak coupling constants by

$$K_{\gamma\gamma\gamma} = \frac{1}{2} g g' (\kappa_1 + 3\kappa_2), \quad (43a)$$

$$K_{Z\gamma\gamma} = \frac{1}{2} [g'^2 \kappa_1 + (g'^2 - 2g^2) \kappa_2], \quad (43b)$$

where $\kappa_{1/2}$ are the parameters defined in [12].

D Standard Model Helicity Amplitudes

Amplitudes with like fermion helicities are zero

$$\mathcal{M}(\sigma_1, \sigma_2, +, +) = \mathcal{M}(\sigma_1, \sigma_2, -, -) = 0 \quad (44)$$

and the SM amplitudes are (cf. also [18])

$$\mathcal{M}_{\text{SM}}(+, -, +, -) = -2ie^2 Q_f^2 \frac{\langle p_2 k_1 \rangle \langle p_1 k_2 \rangle^*}{\langle p_1 k_2 \rangle \langle p_1 k_1 \rangle^*} \quad (45a)$$

$$\mathcal{M}_{\text{SM}}(+, -, -, +) = -2ie^2 Q_f^2 \frac{\langle p_1 k_1 \rangle \langle p_2 k_2 \rangle^*}{\langle p_1 k_2 \rangle \langle p_1 k_1 \rangle^*}. \quad (45b)$$

The combinations with the reversed $(-, +)$ photon polarizations are determined from the $(+, -)$ combination by interchanging k_1 and k_2 .

References

- [1] N. Seiberg, E. Witten, JHEP **9909** (1999) 032 [arXiv:hep-th/9908142].
- [2] S. Minwalla, M. Van Raamsdonk, N. Seiberg, JHEP **0002** (2000) 020 [arXiv:hep-th/9912072].
- [3] J. Gomis, T. Mehen, Nucl. Phys. **B591** (2000) 265 [arXiv:hep-th/0005129]; D. Bahns, S. Doplicher, K. Fredenhagen, G. Piacitelli, Phys. Lett. **B533** (2002) 178 [arXiv:hep-th/0201222]; Yi Liao, K. Sibold, Eur. Phys. J. **C25** (2002) 479 [arXiv:hep-th/0206011]; T. Ohl, R. Rückl, J. Zeiner, Nucl. Phys. **B676** (2004) 229 [arXiv:hep-th/0309021].
- [4] I. Hinchliffe, N. Kersting, Phys. Rev. **D64** (2001) 116007 [arXiv:hep-ph/0104137].
- [5] J. L. Hewett, F. J. Petriello, T. G. Rizzo, Phys. Rev. **D64** (2001) 075012 [arXiv:hep-ph/0010354]; S. Godfrey, M. A. Doncheski, Phys. Rev. **D65** (2002) 015005 [arXiv:hep-ph/0108268]; S. Godfrey, M. A. Doncheski, Talk at the *10th International Conference on Supersymmetry and Unification of Fundamental Interactions (SUSY02), Hamburg, Germany, 17-23 Jun 2002*, [arXiv:hep-ph/0211247].
- [6] J. Wess, Commun. Math. Phys. **219** (2001) 247.
- [7] L. Bonora, M. Schnabl, M. M. Sheikh-Jabbari, A. Tomasiello, Nucl. Phys. **B589** (2000) 461 [arXiv:hep-th/0006091].
- [8] X. Calmet, B. Jurčo, P. Schupp, J. Wess, M. Wohlgenannt, Eur. Phys. J. **C23** (2002) 363 [arXiv:hep-ph/0111115]; X. Calmet, M. Wohlgenannt, Phys. Rev. **D68** (2003) 025016 [arXiv:hep-ph/0305027].
- [9] T. Ohl, J. Reuter, in preparation.
- [10] P. Schupp, J. Trampetic, J. Wess, G. Raffelt, [arXiv:hep-ph/0212292].
- [11] J. Trampetič, Acta Phys. Polon. **B33** (2002) 4317 [arXiv:hep-ph/0212309]; P. Schupp, J. Trampetič, [arXiv:hep-ph/0405163].
- [12] N. G. Deshpande, X.-G. He, Phys. Lett. **B533** (2002) 116 [arXiv:hep-ph/0112320]; W. Behr, N. G. Deshpande, G. Duplančić, P. Schupp, J. Trampetič, and J. Wess, Eur. Phys. J. **C 29** (2003) 441 [arXiv:hep-ph:0202121]; G. Duplančić, P. Schupp, J. Trampetič, Eur. Phys. J. **C 32** (2003) 141 [arXiv:hep-ph/0309138].

- [13] A. Alboteanu, T. Ohl, in preparation.
- [14] K. Hagiwara et al. (Particle Data Group), Phys. Rev. D **66** (2002) 010001.
- [15] B. Badelek et al., *TESLA: The Superconducting Electron Positron Linear Collider With An Integrated X-Ray Laser Laboratory. Technical Design Report. Part 6. Appendices. Chapter 1. Photon Collider At Tesla.*, [arXiv:hep-ex/0108012].
- [16] I. F. Ginzburg, G. L. Kotkin, V. G. Serbo, V. I. Telnov, JETP Lett. **34**, 491 (1981); Nucl. Instrum. Meth. **205** (1983) 47; I. F. Ginzburg, G. L. Kotkin, S. L. Panfil, V. G. Serbo, V. I. Telnov, Nucl. Instrum. Meth. A **219** (1984) 5.
- [17] F. A. Berends, W. Giele, Nucl. Phys. **B294** (1987) 700; S. Dittmaier, Phys. Rev. **D59** (1999) 016007 [arXiv:hep-ph/9805445].
- [18] R. Gastmans, T. T. Wu, *The Ubiquitous Photon – Helicity Method for QED and QCD* (Oxford UP, 1990).
- [19] R. Penrose, W. Rindler, *Spinor Calculus and Twistor Geometry* (Addison-Wesley, 1995), pp. 147ff, 312ff.
- [20] T. Ohl, *O’Mega: An Optimizing Matrix Element Generator*, in *Proceedings of 7th International Workshop on Advanced Computing and Analysis Techniques in Physics Research (ACAT 2000)* (Fermilab, Batavia, IL, 2000) [arXiv:hep-ph/0011243]; M. Moretti, T. Ohl, J. Reuter, [arXiv:hep-ph/0102195]; T. Ohl, J. Reuter, C. Schwinn, *O’Mega* (long write-up, in preparation).
- [21] T. Ohl, Comput. Phys. Commun. **101** (1997) 269 [arXiv:hep-ph/9607454]; T. Ohl, *Circe 2.0 Beam Spectra for Simulating Linear Collider and Photon Collider Physics*, WUE-ITP-2002-006.
- [22] V. Telnov, private communication.